Synthesis and Conformational Transition of Surface-Tethered Polypeptide: Poly(L-lysine)

Yuli Wang and Ying Chih Chang*

Department of Chemical Engineering and Materials Science, University of California, Irvine, California 92697-2575

Received January 24, 2003; Revised Manuscript Received June 4, 2003

ABSTRACT: Poly(L-lysine) (PLL) was end-grafted onto silicon oxide surfaces to study its conformational transition among α-helix, *β*-sheet, and random coil at the solid−water interface. Surface-grafted PLL films were prepared from surface-grafted poly(N^{ϵ}-carbobenzyloxy-L-lysine) (PCBL) thin films, which were fabricated by the surface-initiated vapor-deposition polymerization (SI-VDP) of *N*-carboxyanhydride (NCA) of N^{ϵ}-carbobenzyloxy-L-lysine. The reaction parameters during the SI-VDP process, including NCA concentration, substrate temperature, and reaction time, were optimized in order to synthesize homogeneous PCBL films with well-controlled thickness. Under the optimal conditions (substrate temperature at 105 °C, NCA evaporating temperature at 100 °C, and 8 mg of NCA at 0.1 Pa), α-helical PCBL films with thickness ranging from 4 to 120 nm can be synthesized by controlling the reaction time from 5 to 120 min. The conversion from PCBL to PLL was accomplished by removing N^{ϵ}-carbobenzyloxy groups in the hydrogen bromide/benzene solution with the aid of ultrasonication for 40 min. The surface-grafted PLL films with an estimated DP of 750 exhibited versatile conformations among α-helix, *β*-sheet, and random coil depending on the external environments. The conformational transition from one state to another was successfully induced by external stimuli, such as pH (H^+/OH^-), surfactant (sodium dodecyl sulfate (SDS)), and anion (ClO_4^-). In the process of the conformational transition, macroscopic properties such as thickness, refractive index, and wettability changed correspondingly. For example, a surface-grafted random-coiled PLL had a film thickness of 215 nm and a refractive index of 1.37 at pH 7, whereas it changed to a *β*-sheet conformation when binding with SDS, with the film thickness shrinking to 145 nm and the refractive index increasing to 1.45. Compared to the free PLL chains, the stability of the helical state increased when the PLL chains were densely immobilized on the surfaces. The transitional behaviors were characterized by Fourier transform infrared spectroscopy, circular dichroism spectroscopy, and ellipsometry.

1. Introduction

Surface-grafted synthetic polypeptides have drawn considerable attention in recent years because of their distinct secondary structures (such as α-helix, *β*-sheet, and random coil) and the conformational transitions among these structures. The ordered structures offer unique thin film properties, thus being useful in creating functional surfaces.[1−3] The conformational transition occurred in the films, allowing their applications as stimuli-responsive surfaces.[4−7]

A series of studies have been conducted in our laboratory on the synthesis and conformational properties of several surface-grafted polypeptides, including poly(L-glutamic acid) (PLGA), poly(L-lysine) (PLL), poly(*γ*-methyl L-glutamate), etc. The polypeptides selected in these studies have a common character; i.e., their secondary structures are subject to change in response to external stimuli. Hence, they are quite suitable to be used as surface-responsive materials for applications in sensing and actuating. In the first paper of this series, a surface-grafted PLGA monolayer was obtained by the hydrolysis of the *γ*-benzyl ester groups of the surface-grafted poly(*γ*-benzyl L-glutamate) (PBLG); its α-helical backbone converted to random coil when the neutral acidic side chains changed to the negatively charged forms by the external stimuli.[7]

This is the second paper in this series. In this report, we will focus on the discussion of surface-grafted PLL films. PLL is an important water-soluble polypeptide composed of naturally occurring L-lysine, which contains amine groups on the side chains. PLL can exist among three types of conformations, i.e., α-helix, *β*-sheet, and random coil, depending on the external environments (e.g., solvents and temperatures).[8−10] The conformational transition of the free-chain PLL in solutions has been studied quite extensively in the past. It has shown that conformational transitions can be induced by various external stimuli, including pH,[11,12] surfactants,[13−16] anions,[17−22] polyanions,[23−26] solvents,[27,28] heat,[29,30] mechanical shear force,[31] etc. In addition, PLL has provided functions in gene delivery vectors,[32,33] biomimetic mineralization,[34,35] cell attachment,[36] and biosensors and biosensor arrays.[37] Conceivably, surface-grafted PLL has many interesting properties, and its conformational transition might function to switch on/off such properties; however, neither the synthesis of surface-grafted PLL nor its conformational transitions at surfaces have been reported.

This study thus consists of two parts: (1) Development and optimization of the fabrication approach to synthesize end-grafted PLL films on solid substrates: First, a surface-grafted poly(N^{ϵ}-carbobenzyloxy-L-lysine) (PCBL) film is synthesized by the "surface-initiated vapor-deposition polymerization" (SI-VDP) of "*N*-carboxyanhydride (NCA) of N^{ϵ}-carbobenzyloxy-L-lysine (CBL)" (the monomer is denoted as "CBL-NCA").[38] Second, PCBL is converted to PLL by the deprotection reaction that removes the N^{ϵ}-carbobenzyloxy groups on the side chains. (2) Demonstration of the conformational transitions of surface-grafted PLL and the association with the changes in surface properties. In particular, pH (H^+/OH^-), surfactant (sodium dodecyl sulfate (SDS)),

10.1021/ma034093r CCC: $25.00
Published on Web 08/02/2003

Scheme 1. Schematic Diagram Showing the Conformational Transition among α-Helix, *β*-Sheet, and Random Coil Induced by External Stimuli for a Surface-Grafted PLL Thin Film[a]

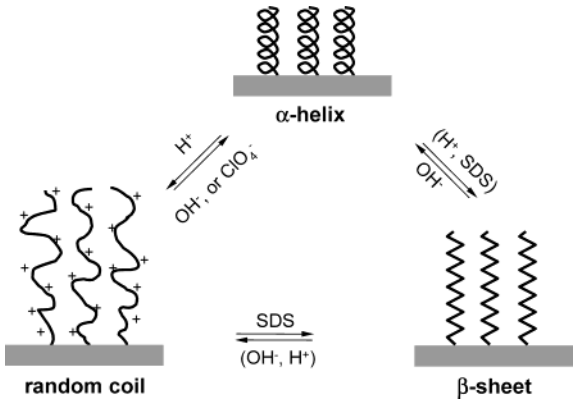

[a] (H^+, SDS) means treating the film successively with H^+ and SDS.

and anion (ClO_4^-) are used as the external stimuli. The anticipated conformational transitions among α-helix, *β*-sheet, and random coil induced by these stimulants are summarized in Scheme 1. Circular dichroism (CD) and Fourier transform infrared spectroscopy (FTIR) are used to characterize the conformations in films. Ellipsometry is applied to measure the dimensional changes of surface-grafted films in response to the conformational changes.

2. Experimental Section

2.1. Synthesis of Surface-Grafted PLL. Scheme 2 outlines the three-step pathway to synthesize a surface-grafted PLL on silicon and quartz substrates. The detailed information about chemicals, cleaning of substrates and debenzylation, is described in the Supporting Information.

(1) Vapor silanization of the substrates with 3-(aminopropyl)triethoxysilane (APS) initiator layer.[38]

(2) SI-VDP of CBL-NCA: The SI-VDP process was carried out by using the reaction setup described in the previous publication.[38] The NCA evaporating temperature was fixed at 100 °C, and the vacuum was maintained below 0.1 Pa. Other reaction parameters including the amount of NCA, substrate temperature, and reaction time were optimized for the PCBL system. (Throughout the context, the two temperature settings will be expressed as, for example, 105 °C/100 °C, to indicate the operating substrate temperature at 105 °C and NCA evaporating temperature at 100 °C.) After the completion of the reaction, the substrates were sonicated in a mixture of dichloroacetic acid (DCA) and chloroform (20/80 (v/v)) for 5 min, followed by rinsing with fresh chloroform and drying under a stream of nitrogen.

(3) Conversion of surface-grafted PCBL to PLL: The surface-grafted PCBL films were sonicated in the HBr/benzene solution for 40 min to remove N^{ϵ}-carbobenzyloxyl protection groups.[7] After the reaction, the substrates were rinsed with toluene, acetone, and distilled water and dried under a stream of nitrogen.

2.2. Characterization Methods.[7] FTIR was used to characterize the polypeptide films on silicon substrates. CD was used to in situ measure the conformation of the polypeptide films on quartz plates. An ellipsometer was used to in situ characterize the solvated film at the water−solid interface during the conformational transitions. The detailed information about characterization methods is described in the Supporting Information.

3. Results and Discussion

3.1. Optimization of the SI-VDP Conditions for the Synthesis of Surface-Grafted PCBL. The first example of the synthesis of surface-grafted PCBL with thickness of 99.3 ± 0.3 nm by the SI-VDP process has been demonstrated in our previous publication.[38] In that particular case (both substrate and NCA evaporating temperatures were at 102 °C, under 0.1 Pa for 30 min), only the NCA evaporating temperature and pressure were optimized. In this report, we have investigated other synthetic parameters, including monomer concentration, substrate temperature, and reaction time, to further identify the optimal reaction conditions.

Scheme 2. Schematic Diagram of the Synthetic Pathway for the Surface-Grafted PLL Thin Film[a]

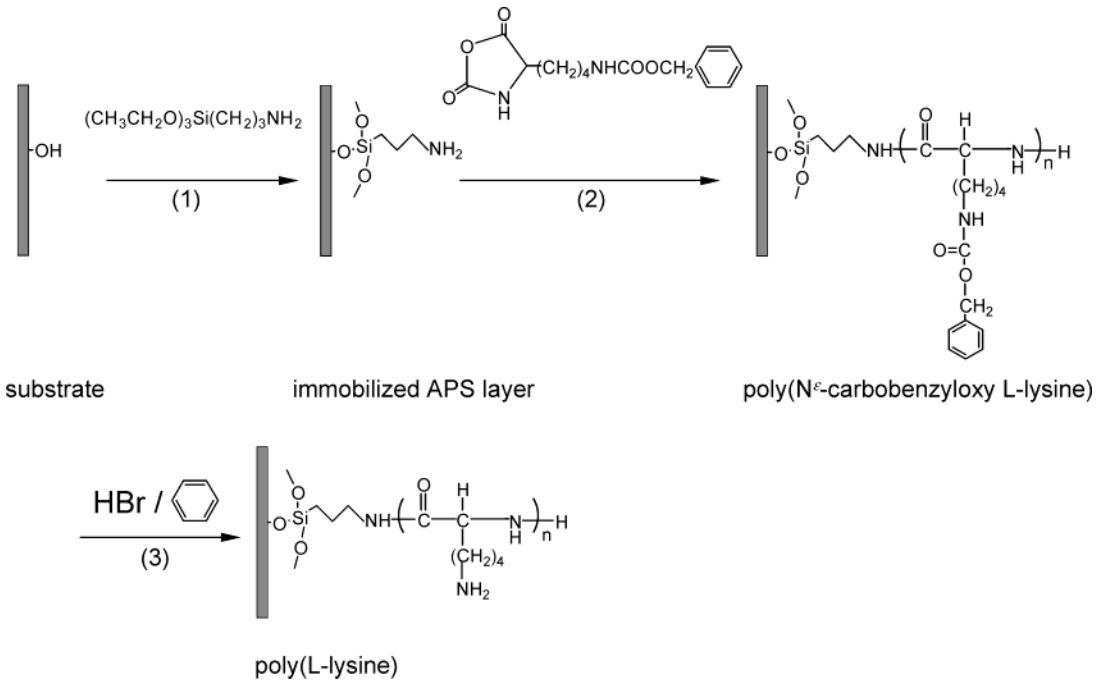

[a] (1) Vapor silanization of the substrate by APS; (2) SI-VDP of CBL−NCA from the surface-bound APS layer; (3) cleavage of N^{ϵ}-carbobenzyloxy groups of the surface-grafted PCBL to form PLL.

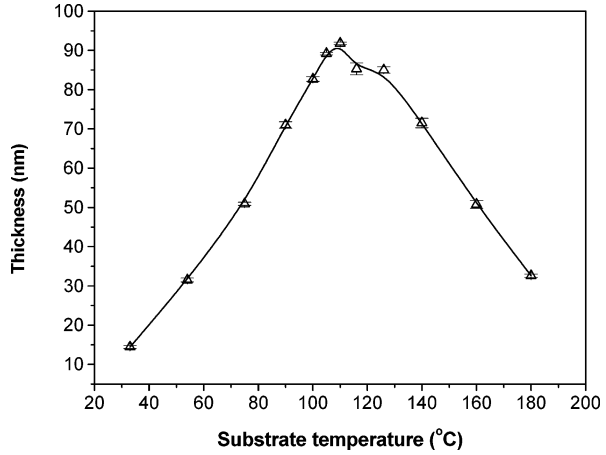

Figure 1. Dependence of the PCBL fim thickness on the substrate temperature. Reaction conditions: 100 °C NCA evaporating temperature, 8 mg of CBL−NCA, and 30 min reaction time.

3.1.1. Monomer Concentration. We found that the initial CBL-NCA quantity should be between 7 and 9 mg to synthesize the thickest possible film (the results are not shown here). Hence, throughout this report, 8 mg of CBL-NCA will be used unless otherwise noted; this quantity corresponds to the 0.015 mol/L vapor concentration for the particular chamber dimensions (internal dimensions: diameter × width × height = 33 × 13 × 4 mm) we used.[38]

3.1.2. Substrate Temperature. To verify the substrate temperature effect on the surface polymerization, we studied the dependence of PCBL film thickness on the substrate temperature, as shown in Figure 1. For the polymerization at 100 °C evaporating temperature for 30 min, the substrate temperatures were changed from 32 to 180 °C. Consequently, the thickness of the resulting films varied widely from 14 nm (at 32 °C) to 90 nm (between 105 and 110 °C). This parabolic plot is similar to the finding of the grafting of PBLG,[38] suggesting that two competing factors dominate the growth of film thickness: (1) The surface reactivity and the effective vapor concentration of monomers increased with the substrate temperature. (2) The randomization of surface-grafted chains increased with the substrate temperature (i.e., the molecular chains become less accessible to the subsequent polymerization). These two competing factors result in an optimal substrate temperature around 105 °C, at which the thickest PCBL film can be synthesized.

3.1.3. Reaction Time. Figure 2 shows the PCBL growth as a function of time at one of the optimal conditions (i.e., 105 °C/100 °C). Without consuming all NCA monomers, the PCBL growth reaches a plateau after 55 min of reaction time with the thickness of 114 nm, due to the surface blockage of excess monomers. The standard deviation of ellipsometric thickness is typically in the range 0.4−1.2 nm for all 12 samples used in Figure 2 (for each sample, at least 10 measurements in 1 × 1 cm^2 area). This indicates that the surface-grafted PCBL films fabricated by the SI-VDP method are smooth and homogeneous. In fact, the samples appear to be clean and reflective, and we can discern different thickness by the reflective lights—it appears to be gray around 30 nm, dark around 50 nm, and blue above 90 nm.

Figure 2 can be used as the calibration standard to fabricate PCBL films with desirable film thickness

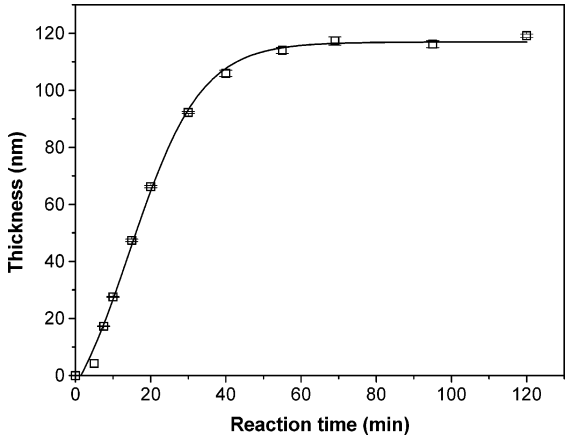

Figure 2. Growth of surface-grafted PCBL films monitored by ellipsometry. Reaction conditions: 100 °C/105 °C with 8 mg of CBL−NCA.

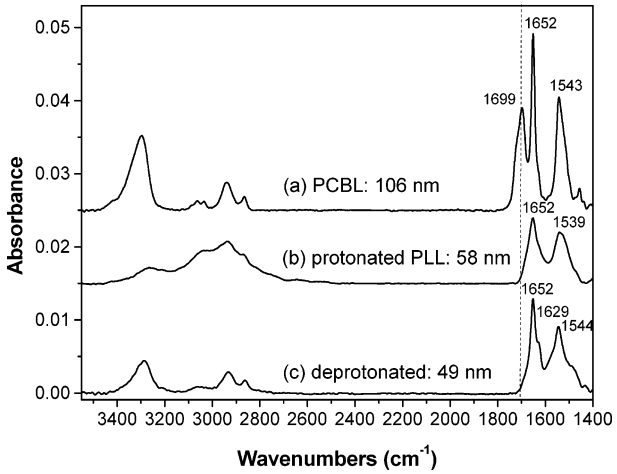

Figure 3. FTIR spectra of surface-grafted (a) PCBL, (b) protonated PLL dried from pH 2, and (c) deprotonated PLL dried from pH 11. The PCBL was grown on silicon substrates. The thickness of the dried film is labeled above each spectrum.

reliably from 4 to 119 nm.

For the following context, all the PCBL samples later converted to PLL were fabricated at the same reaction conditions (105 °C/100 °C with 8 mg of CBL-NCA for 40 min). Ellipsometric measurements for the samples grafted on silicon wafers show the obtained film thickness of 106.1 ± 0.9 nm and refractive index of 1.557 ± 0.001. From FTIR (Figure 3a), the amide I absorption peak at 1652 cm^{-1} and the amide II at 1543 cm^{-1} indicate the α-helical conformation. From CD (Figure 4a), the double minima at 210 and 223 nm and the maximum at 193 nm also confirm a typical α-helical conformation. The α-helical conformation found in the grafting state is consistent with the previous finding of free-chain PCBL, mainly due to the shielding effects from the bulky side chains, and only helix-breaking solvents, such as trifluoroacetic acid and *m*-cresol, were able to disrupt its regular structure.[39]

3.2. Surface-Grafted PLL Films in Air. To be converted to PLL, the N^{ϵ}-carbobenzyloxy groups of surface-grafted PCBL films were removed by anhydrous HBr in benzene with the aid of 40 min sonication. The completion of deprotection reaction was confirmed by FTIR. The FTIR spectra of the resulting films in both protonated (with $-NH_3^+$ ionized side chains) and deprotonated (with $-NH_2$ neutral side chains) forms (Figure 3b,c) are compared with their precursor, the PCBL film

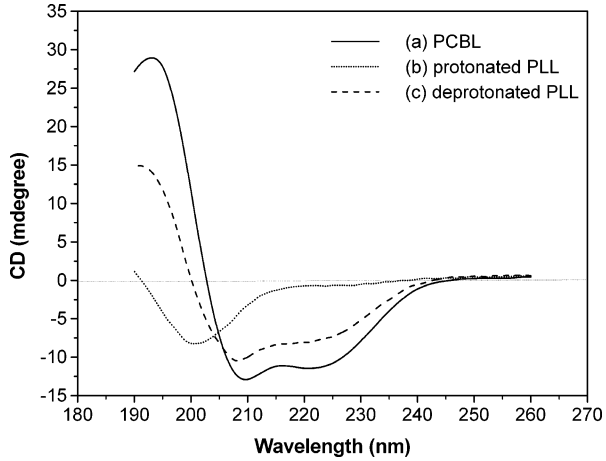

Figure 4. CD spectra of surface-grafted (a) PCBL, (b) protonated PLL, and (c) deprotonated PLL. The PCBL was grown on quartz substrates. The SI-VDP and deprotection conditions were the same as those grown on silicon substrates shown in Figure 3.

Table 1. Ellipsometric Measurements and Water Contact Angles of Surface-Grafted PCBL and PLL

samples	thickness in dry film (nm)	refractive index in dry film	contact angle (deg)
PCBL	106.1 ± 0.9	1.557 ± 0.001	62 ± 2
protonated PLL	57.8 ± 0.5	1.510 ± 0.002	8 ± 2
deprotonated PLL	49.4 ± 0.2	1.500 ± 0.002	42 ± 4

(Figure 3a). The complete removal of protection groups is verified by the total disappearance of the carbobenzyloxy absorption peak originally presented at 1699 cm^{-1}.

3.2.1. Spectroscopic Studies of Secondary Structures of PLL Films. The protonated PLL sample, prepared by treating the sample with a pH 2 buffer (in this study, all the buffers were prepared by 5 mM bis-tris-propane), has the amide I at 1652 cm^{-1} and the amide II at 1539 cm^{-1} measured in air. On the other hand, the deprotonated PLL, prepared by treating with a pH 11 buffer, has the amide I at 1652 cm^{-1} and the amide II at 1544 cm^{-1}. The small shoulder at 1629 cm^{-1} in the deprotonated PLL spectrum suggests that a trace of β-sheet structure is spontaneously formed under high-pH conditions at room temperature.[40] The amide I peak of the deprotonated PLL is sharper than that of the protonated one. Despite these subtle differences between the two spectra, it is difficult to discern the secondary structures of both protonated and deprotonated samples by FTIR because the amide I absorption peaks attributed by helix and random coil are not distinguishable with only few wavenumber shifts.

The secondary conformations formed at protonated and deprotonated states are further characterized by CD. In Figure 4b,c, we found that the deprotonated PLL sample adopts an α-helical conformation, while the protonated PLL adopts a random-coil conformation, evidenced by the negative peak at 200 nm. Overall, FTIR measurement is ideal for identifying the chemical compositions of the surface films, while CD is better for discerning helices and random coils.

3.2.2. Surface Properties of Grafted PLL vs PCBL Films. The film properties, including thickness, refractive index, and wettability, change significantly when PCBL is converted to PLL, as summarized in Table 1. The static water contact angle of PCBL films is 62°. The removal of N^{ϵ}-carbobenzyloxy groups decreases the hydrophobicity. Depending upon the degree of protonation of the amine side groups, the surface hydrophobicity of PLL differs: Deprotonated PLL film has a contact angle of 42°, whereas the protonated one is almost completely hydrophilic with a contact angle as small as 8° due to electrostatic interactions.

Simultaneously, the conversion of PCBL to PLL decreases both film thickness and refractive index from 106 nm (PCBL) to 58 nm (protonated PLL) and 49 nm (deprotonated PLL), with refractive index from 1.58 (PCBL) to 1.51 (protonated PLL) and 1.50 (deprotonated PLL). The removal of bulky N^{ϵ}-carbobenzyloxy groups provides unoccupied space in films. In addition, despite the mild condition we adopted in the deprotection treatment, the possibility of partial film depletion cannot be excluded completely. These two factors attribute to the decrease of film thickness from PCBL to PLL films. The changes of film thickness and refractive index of the PLL film in the protonated and deprotonated states, on the other hand, could be attributed to their different secondary structures. The α-helical conformation in the deprotonated state has a relatively compact structure (49 nm) than the random-coil conformation in the protonated state (58 nm).

So far, we only discuss the properties of dry films after different pH treatments; in the following sections, we will focus on the in-situ studies of the film properties in various environments.

3.3. Overview: Conformational Transitions of Surface-Grafted PLL Induced by External Stimuli. PLL is an interesting polypeptide material capable of converting its secondary structures among α-helix, β-sheet, and random coil, depending upon its surroundings. Previous studies in free-chain PLL have found that when the PLL is protonated in a neutral or acidic pH solution, it adopts a random-coil conformation because of the electrostatic repulsion among the side chains. On the contrary, at alkaline pH, the deprotonated PLL is capable of forming regular α-helix structures with intramolecular hydrogen bonds between repeating units i and $i + 3$. Interestingly, the helical structure would further convert to β-sheet structure at either extremely high pH[41] or high temperature.[8]

In the presence of selected low molecular weight ionic species, the conformation transitions alter. For example, conversion from random-coil to α-helix at neutral pH is facilitated by the presence of potassium thiocyanate,[17,18] sodium perchlorate,[17,19−21] or sodium carbonate,[22] when the salt concentration is on the order of 0.1−1.0 M. At a much lower concentration of 10^{-4} M, anionic surfactants can induce the conversion from random-coil to either β-sheet (by SDS[13,14]) or α-helix (by sodium octyl sulfate[15]) at neutral pH.

When the PLL chains are tethered to a surface through the one-point attachments, we anticipate that the grafting chains would undergo conformational transitions differently due to the reduced degree of freedom for the chain movement. In this study, we will first investigate the conformational coil−helix−sheet transition with the increase of pH (H^+/OH^-). Second, the coil−sheet transition will be studied by adding a large surfactant molecule, SDS. Third, the coil−helix transition in neutral pH will be examined by adding a small anionic species, ClO_4^-.

3.4. Coil−Helix−Sheet Transition Induced by pH. We used both CD and ellipsometry to measure the helix−coil−sheet transition in the surface-grafted PLL

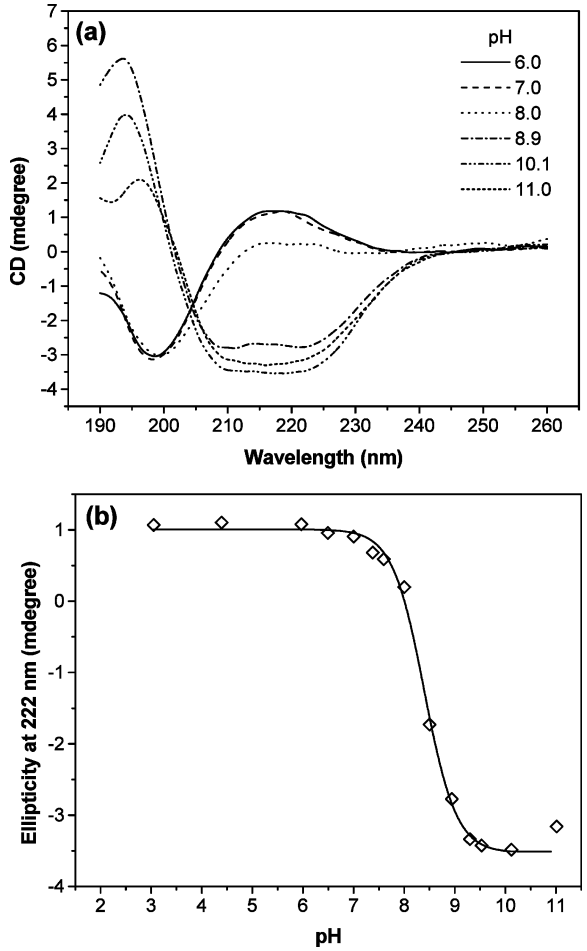

Figure 5. (a) CD spectra of a surface-grafted PLL on a quartz plate in 5 mM bis-tris-propane buffer from pH 3 to pH 11. (b) pH dependence of CD ellipticities at 222 nm.

film induced by pH.

3.4.1. CD Measurements. Figure 5a shows the CD spectra of a surface-grafted PLL film on a quartz substrate in the aqueous solution with pH from 6 to 11. At pH lower than 7, the CD spectra show the random-coil conformation, with a maximum centered at 217 nm and a minimum at 198 nm. At pH higher than 9, the CD spectra show double minima at 210 and 222 nm and a maximum at 193 nm, which is typical for the α-helical conformation. The ellipticity at 222 nm is used as a measure of helical content. Figure 5b is the plot of ellipticity at 222 nm as a function of pH. It clearly shows that the coil−helix transition taken place within 1.5 pH difference with the transitional point pH_t at 8.4.

3.4.2. Ellipsometry. Figure 6 is the plot of thickness and refractive index of a surface-grafted PLL on a silicon substrate against pH. The transition observed from both thickness and refractive index occurs between pH 7.5 and pH 9.2. The thickness decreases from 207 nm at pH 7 to 113 nm at pH 10, when the refractive index increases from 1.37 to 1.41. The transitional point pH_t is 8.4. The pH-induced film thickness and refractive index changes match the helix−coil transition as observed from CD spectra.

Following the same way we used in our previous publication,[7] we can estimate the DP of surface-grafted PLL by ellipsometric thickness. In the pH 9.5 buffer, PLL has 100% helical conformation, and its helical chains are vertical oriented due to the interaction between PLL and water. The average length of each

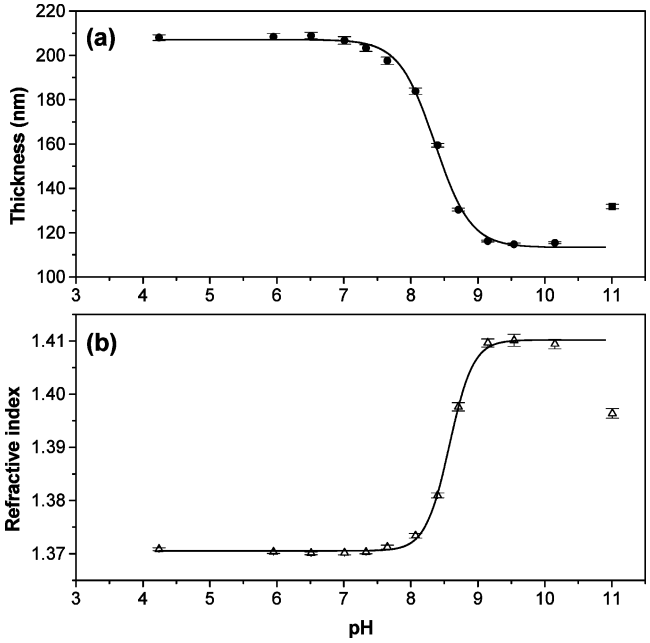

Figure 6. pH denpendence of the (a) ellipsometric thickness (b) and refractive index of a surface-grafted PLL (DP = 750) on a silicon substrate from pH 4 to pH 11 in 5 mM bis-tris-propane buffer.

repeating unit is 0.15 nm for helical chain and 0.35 nm for random-coiled chain.[42] Therefore, for the end-grafted PLL in this study, the DP = d_H/0.15 = 113/0.15 = 750 and $M_w \sim 2.0 \times 10^5$, where d_H is the measured thickness at helical conformation (i.e., in the pH 9.5 buffer).

For PLL with DP of 750, thickness at random coil (d_C) at pH 7 should be 0.35DP = 263 nm if the random-coiled chains are full extended. However, the actually measured thickness at pH 7 is 207 nm. Therefore, $d_C = (0.35DP)^{0.96}$. It suggests that random-coiled PLL chain is not fully extended from the surface. This result is consistent with the PLGA system, where $d_C = (0.35DP)^{0.93}$.[7]

When the pH continues to increase up to 11, a third conformation seems to appear. From CD, only one minimum at around 216 nm is displayed, indicating a β-sheet structure (Figure 5a). From ellipsometry, the film thickness arises abruptly to 132 nm, also indicating expanded molecular chains (Figure 6a). Compared to the free-chain PLL, where the spontaneous β-sheet formation was experienced only for the concentrated PLL samples (>25−50 mg/mL) at pH 11 solution for at least 2 h,[43] the β-sheet formation in the grafting state is instantaneous (less than detectable time, i.e., seconds). This β-sheet formation has been ascribed to the association of lysyl side chains, which contain four apolar methylene groups. In the grafting state, we hypothesize that the relatively organized and highly concentrated PLL near surface reduce the degree of freedom of forming β-sheet structure.

3.4.3. Equivalency of CD and Ellipsometry. Figure 7 shows f_H (and f_C) vs pH plots for both measurements, where f_H is the fraction of helix from CD measurements and f_C is the degree of compression from ellipsometric measurements.[7] These two curves are almost coincident. This finding suggests that the compression/expansion of the grafted PLL films is primarily induced by the conformational transition.

Surface-grafted PLGA has been investigated as a pH-sensitive gating to regulate water permeability, with the

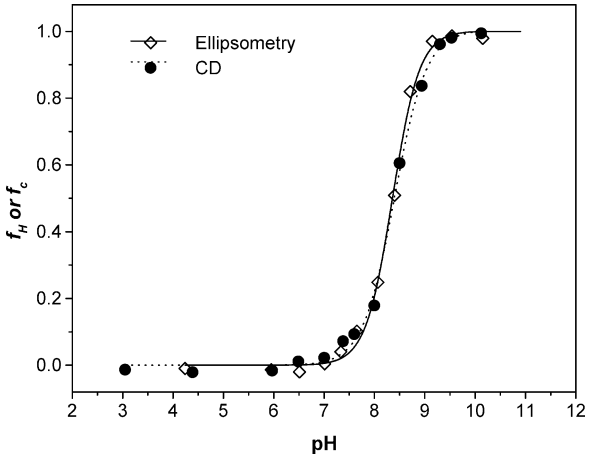

Figure 7. Equivalency of CD and ellipsometry in studying the pH-induced coil-to-helix transition for the surface-grafted PLL (DP = 750). A silicon substrate was used in ellipsometry, and a quartz substrate was used in CD.

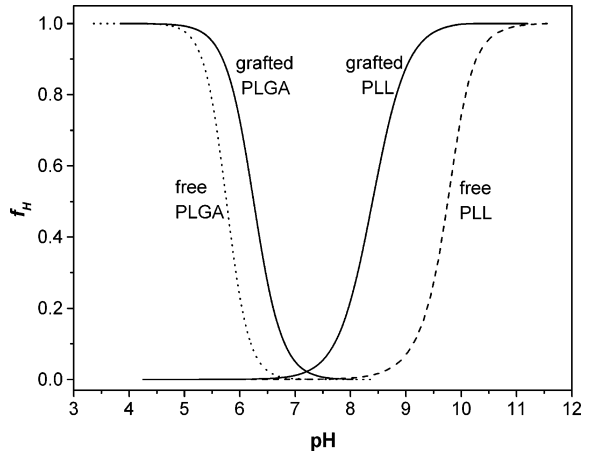

Figure 8. Comparison of the helix−coil transitional behavior in the surface-grafting and free solution state. Only trend lines obtained from CD measurements are shown here. For PLGA system, 2 mM sodium phosphate buffers were used; for PLL system, 5 mM bis-tris-propane buffers were used. Surface-grafted PLGA has an estimated DP of 1100 ($M_w \sim 1.4 \times 10^5$) and surface-grafted PLL has an estimated DP of 750 ($M_w \sim 2.0 \times 10^5$). Free PLGA has M_w of 15 000−50 000, and free PLL has M_w of 30 000−70 000 (both free-chain PLGA and PLL were purchased from Sigma-Aldrich).

open/close point at around pH 6.[4,5] Conversely, the correlation between thickness and conformational transition in the grafted PLL film indicates a new type of pH-gating, with the close/open point at pH 8.4. Interesting application such as cografting PLGA and PLL can create a "smart" pH gating, where the gate closes at neutral pH (pH 6−8.4) when both PLGA and PLL expand (in random-coil form) and opens at both low and high pH when one of them compresses (in helix form).

3.4.4. Comparison of Transition between Surface-Grafting State and Free State. The association constant for the ϵ-amino group of PLL is reported as $pK_a = 10.0-10.3$ at 25 °C in 0.1 M KCl.[44] For the free-chain PLL in solution, the pH-induced coil-to-helix transitional inflection point, pH_t, is about 9.7. In contrast, for the surface-grafted PLL, the transitional point pH_t shifts to the acidic side, i.e., pH 8.4 (see Figure 8). In the previous study in the PLGA system, the pH_t is at 5.74 for the free chains and shifts to 6.25 for the grafting chains.[7] Thus, the results from both PLGA and PLL suggest that the helical conformation is favorable in the grafting

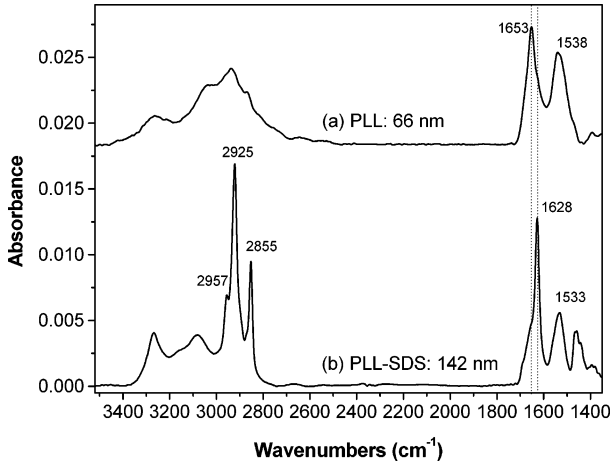

Figure 9. FTIR spectra of a surface-grafted dry (a) protonated PLL (66 nm) and (b) PLL−SDS complex (142 nm). To prepare the PLL−SDS complex, the PLL film was immersed in 10 mM SDS solution (buffered by 5 mM pH 7 bis-tris-propane) for 20 min and taken out and rinsed by distilled water and dried by a stream of nitrogen.

state. The additional free energy involved in surface-grafting state contributes to the shift of transitional point pH_t from free state to surface-grafting state. In other words, when the PLL chains are densely immobilized on the surfaces, the stability of the helical state is reinforced. Our experimental data are consistent with the prediction from Buhot's model, although it was based on the thermally induced helix−coil transition of the surface-grafted neutral polypeptides.[45]

3.5. Coil-to-β Transition Induced by Surfactant (SDS). Free-chain PLL is known to form a β-sheet structure when binding with the anionic surfactant SDS.[13,14] It is ascribed to the hydrophobic interaction among the bound surfactant molecules, which overshadows the electrostatic interaction.

When the PLL molecules are immobilized on a solid surface, the coil-to-β transition also occurs at the interface. Figure 9 shows the FTIR spectra of the surface-grafted PLL and PLL−SDS complex in dry films, with the thickness labeled above each spectrum. Figure 9a is the spectrum of a random-coiled PLL which dried from pH 7 buffer, with a broad amide I absorption peak at 1653 cm^{-1}. Figure 9b is the spectrum of the same sample after binding with SDS. The complexation of SDS to PLL is evident: The dry film thickness increases from 66 nm for deprotonated PLL to 142 nm for PLL−SDS complex; the absorption peaks of PLL−SDS complex at 2957 (weak, CH_3, asym, stretch), 2925 (strong, alkyl CH_2, asym, stretch), and 2855 cm^{-1} (strong, alkyl CH_2, sym, stretch) come from the alkyl chains of SDS. Both shifts of the amide I and amide II bands indicate the transition of secondary conformations: The amide I changes from 1653 to 1628 cm^{-1}, while amide II changes from 1533 to 1538 cm^{-1}. Both indicate that PLL−SDS complex in dry state adopts a β-sheet conformation.

The coil-to-β transition caused by binding with SDS can further be affirmed by CD. In addition, it has an advantage over FTIR in that it can measure the real conformations in the aqueous environment. Figure 10 shows the CD spectra of PLL before and after binding with SDS in a pH 7 buffer. The spectrum in the absence of surfactant represents a random-coil conformation, which is characterized by two extrema: a maximum centered at 216 nm and a minimum at 200 nm. After

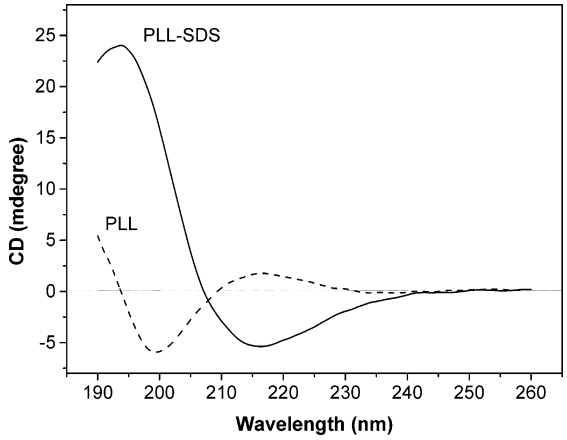

Figure 10. CD spectra of surface-grafted PLL and PLL−SDS complex in 5 mM pH 7 bis-tris-propane buffer.

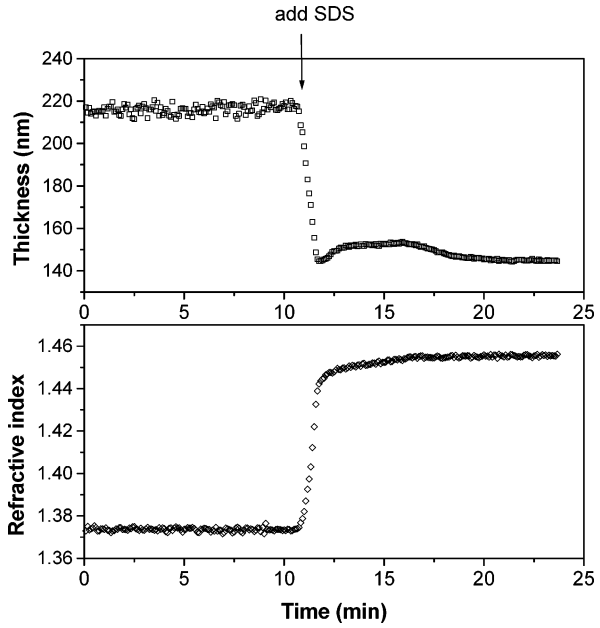

Figure 11. Thickness and refractive index of a surface-grafted PLL in the course of interaction with SDS measured by ellipsometry. A 60 mL aliquot of 5 mM pH 7 bis-tris-propane buffer was added to the liquid cell, followed by an addition of a 1 mL of 10 mM SDS solution at 12 min (indicated as an arrow).

binding with SDS, the CD spectrum has a one minimum at 217 nm and a maximum at 195 nm, suggesting a typical β-sheet conformation.

Ellipsometry was employed to investigate the dimensional and density transitions of PLL when binds with SDS. As mentioned before, ellipsometry provides indirect evidence about the conformational transition. Figure 11 shows the change of the film thickness and refractive index of a surface-grafted PLL during the SDS binding. Before the binding, the PLL film adopts random-coil conformation, with a film thickness of 217 nm and a refractive index of 1.37. After the addition of SDS to the liquid cell, the film thickness gradually decreases to 145 nm while the refractive index increases to 1.45. The decrease of the film thickness is due to the change from an extended random-coil conformation for PLL to a relatively compacted β-sheet conformation for PLL−SDS. The increase of refractive index is due to the shrinkage of PLL main chains as well as the binding of long alkyl chains (12 carbons) onto the side groups. The

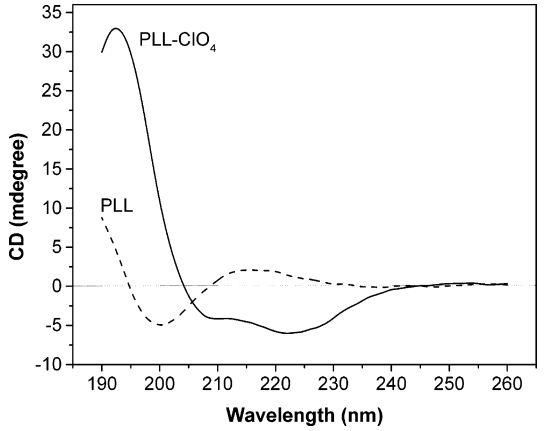

Figure 12. CD spectra of surface-grafted PLL and PLL−ClO_4 complex in 5 mM pH 7 bis-tris-propane buffer indicate the coil-to-helix transition in the formation of the complex.

transition process takes about 3 min. This process is comparatively slower than that induced by pH, which is almost instantaneous. It is partially due to the relative slow diffusion of SDS into the PLL film and partially due to the slow conformational transition of PLL when binding with SDS.

The conformational transition caused by binding of *n*-alkyl surfactant onto ionic polypeptides can be explained by two interactions: one is the electrostatic interaction of side groups, and the other is the hydrophobic interaction between alkyl chains. For the PLL−SDS system, the hydrophobic interaction predominates the electrostatic interaction, promoting β-sheet conformation. It is interesting to compare PLL with the PLGA system, which binds with a cationic surfactant decylammonium chloride decreasing the electrostatic repulsion of side groups, leading to an α-helical conformation instead of β-sheet (hydrophobic interaction seems to be relatively small).[7]

The PLL−SDS complex is stable at the neutral pH condition, however, dissociating at high pH. We found that SDS is removed after treating with pH 11 buffer for 1 min, as evidenced by the disappearance of strong alkyl absorption peaks at 2957, 2925, and 2855 cm^{-1} in FTIR.

3.6. Coil-to-Helix Transition Induced by Anion (ClO_4^-). It is known that ClO_4^- can induce the coil-to-helix transition of solvated PLL molecules at neutral pH[17] as a result of the neutralization of positive charges of the side chains. In our study, we demonstrate the $NaClO_4$ effect on the surface-grafted PLL films. Figure 12 shows the CD spectra of a surface-grafted PLL film in the absence and the presence of 2 M ClO_4^- in a pH 7 buffer. In the absence of ClO_4^-, PLL is random-coiled. In complexation with ClO_4^-, the PLL converts to helices as shown by the double minimum at 208 and 222 nm and a maximum at 193 nm.

By comparison, the ion-induced coil−helix transition also takes place in the case of the surface-grafted PLGA, where divalent metal cations (such as Ca^{2+}, Mg^{2+}, Cd^{2+}) were used. In general, the interaction between Ca^{2+} and PLGA is strong compared to that of PLL−ClO_4 complex. We found that the slight heating can dissociate the PLL−ClO_4 complex. For example, in a water−methylformamide (8/2) mixture containing 0.5 M $LiClO_4$, the PLL−ClO_4 complex dissociates at around 30 °C, converting back to coiled conformations.[30]

4. Conclusions

By using SI-VDP of CBL−NCA, surface-grafted PCBL films were synthesized. The reaction parameters, including monomer concentration, substrate temperature, and reaction time, were optimized. It was found that the optimal substrate temperature was between 105 and 110 °C. The film thickness ranging from 4 to 120 nm can be tuned by controlling the reaction time from 5 to 120 min.

The conversion of PCBL to PLL was achieved by removing N^{ϵ}-carbobenzyloxy groups with the anhydrous HBr in benzene solution under 40 min ultrasonication. FTIR, CD, water contact angles, and ellipsometry were used to confirm the full conversion. In addition, these tools were also used to identify the properties of the dry PLL films. It was found that the degree of protonation of the dry films depends on the previous solvent treatment and causes very different properties. (For example, the protonated PLL adopts a random coil conformation and is thicker and more hydrophilic than the helical deprotonated PLL film.)

The stimuli-responsive properties of surface-grafted PLL were demonstrated by the dielectric property changes while converting among α-helix, β-sheet, and random coil. pH (H^+/OH^-), surfactant (SDS), and anion (ClO_4^-) were chosen as the external stimuli. FTIR was used to characterize the conformations of dry films, while CD and ellipsometry were used to measure their in-situ responses. Both CD and ellipsometry gave equivalent results that associate with the helix−coil transition and the dielectric property changes.

Consistent with our observation in the PLGA system, we found that the surface grafting favors the helix state rather than the random coil state, as shown by the shift of the coil-to-helix transition point pH_t to the acidic side. This shift can be ascribed to the additional free energy involved in the surface-grafting state.

In conclusion, the surface-grafted PLL was demonstrated as a new category of responsive, biocompatible materials in that almost 100% change of thickness can be achieved by associating with the coil-to-helix transition under the influence of pH or other proven stimulants. Future applications of this material combined with other grafted polypeptides in the design of smart surfaces, regenerable biosensors, and microfluidic bioanalytical devices are promising and currently under investigation.

Supporting Information Available: Experimental information on (1) chemicals, (2) cleaning of substrates, (3) debenzylation, and (4) characterization methods. This material is available free of charge via the Internet at http://pubs.acs.org.

References and Notes

(1) Jaworek, T.; Neher, D.; Wegner, G.; Wieringa, R. H.; Schouten, A. J. *Science* **1998**, *279*, 57.
(2) Chang, Y.-C.; Frank, C. W.; Forstmann, G. G.; Johannsmann, D. *J. Chem. Phys.* **1999**, *111*, 6136.
(3) Hartmann, L.; Kratzmüller, T.; Braun, H.-G.; Kremer, F. *Macromol. Rapid Commun.* **2000**, *21*, 814.
(4) Ito, Y.; Ochiai, Y.; Park, Y. S.; Imanishi, Y. *J. Am. Chem. Soc.* **1997**, *119*, 1619.
(5) Ito, Y.; Park, Y. S.; Imanishi, Y. *Langmuir* **2000**, *16*, 5376.
(6) Hollman, A. M.; Bhattacharyya, D. *Langmuir* **2002**, *18*, 5946.
(7) Wang, Y.; Chang, Y. C. *Macromolecules* **2003**, *36*, xxxx.
(8) Davidson, B.; Fasman, G. D. *Biochemistry* **1967**, *6*, 1616.
(9) Lotan, N.; Berger, A.; Katchalski, E. *Annu. Rev. Biochem.* **1972**, *41*, 869.
(10) Woody, R. W. *Macromol. Rev.* **1977**, *12*, 181.
(11) Meyer, Y. P. *Macromolecules* **1969**, *2*, 624.
(12) Appel, P.; Yang, J. T. *Biochemistry* **1965**, *4*, 1244.
(13) Satake, I.; Yang, J. T. *Biopolymers* **1975**, *14*, 1871.
(14) Rifkind, J. M. *Biopolymers* **1969**, *8*, 685.
(15) Satake, I.; Yang, J. T. *Biochem. Biophys. Res. Commun.* **1973**, *54*, 930.
(16) Ponomarenko, E. A.; Tirrell, D. A.; MacKnight, W. J. *Macromolecules* **1996**, *29*, 8751.
(17) Puett, D.; Ciferri, A.; Bianchi, E.; Hermans, J. Jr. *J. Phys. Chem.* **1967**, *71*, 4126.
(18) Saito, H.; Ohki, T.; Kodama, M.; Nagata, C. *Biopolymers* **1978**, *17*, 2587.
(19) Peggion, E.; Cosani, A.; Terbojevich, M.; Borin, G. *Biopolymers* **1972**, *11*, 633.
(20) Seipke, G.; Arfmann, H.-A.; Wagner, K. G. *Biopolymers* **1974**, *13*, 1621.
(21) Conio, G.; Patrone, E.; Rialdi, G.; Ciferri, A. *Macromolecules* **1974**, *7*, 654.
(22) Kakiuchi, K.; Akutsu, H. *Biopolymers* **1981**, *20*, 345.
(23) Domard, A.; Rinaudo, M. *Macromolecules* **1981**, *14*, 620.
(24) Schodt, K. P.; McDonnell, M. E.; Jamieson, A. M.; Blackwell, J. *Macromolecules* **1977**, *10*, 701.
(25) Paradossi, G.; Chiessi, E.; Malovìkovà, A. *Macromolecules* **2001**, *34*, 8179.
(26) Hammes, G. G.; Schullery, S. E. *Biochemistry* **1968**, *7*, 3382.
(27) Shepherd, I. W. *Biochem. J.* **1976**, *155*, 543.
(28) Epand, R. F.; Scheraga, H. A. *Biopolymers* **1968**, *6*, 1383.
(29) Müller, M.; Buchet, R.; Fringeli, U. P. *J. Phys. Chem.* **1996**, *100*, 10810.
(30) Ali, S. *Polymer* **1978**, *19*, 229.
(31) Lee, A. T.; McHugh, A. J. *Biopolymers* **1999**, *50*, 589.
(32) Ward, C. M.; Read, M. L.; Seymour, L. W. *Blood* **2001**, *97*, 2221.
(33) Liu, G.; Molas, M.; Grossmann, G. A.; Pasumarthy, M.; Perales, J. C.; Cooper, M. J.; Hanson, R. W. *J. Biol. Chem.* **2001**, *276*, 34379.
(34) Cha, J. N.; Stucky, G. D.; Morse, D. E.; Deming, T. J. *Nature (London)* **2000**, *403*, 289.
(35) Van Bommel, K. J. C.; Jung, J. H.; Shinkai, S. *Adv. Mater.* **2001**, *13*, 1472.
(36) Kranz, B. R.; Thiel, E.; Thierfelder, S. *Blood* **1989**, *73*, 1942.
(37) Strother, T.; Cai, W.; Zhao, X.; Hamers, R. J.; Smith, L. M. *J. Am. Chem. Soc.* **2000**, *122*, 1205.
(38) Wang, Y.; Chang, Y.-C. *Langmuir* **2002**, *18*, 9859.
(39) Matsuoka, M.; Norisuye, T.; Teramoto, A.; Fujita, H. *Biopolymers* **1973**, *12*, 1515.
(40) Pederson, D.; Gabriel, D.; Herman, J. *Biopolymers* **1971**, *10*, 2133.
(41) Wooley, S.-Y. C.; Holzwarth, G. *Biochemistry* **1970**, *9*, 3604.
(42) Nilsson, S.; Zhang, W. *Macromolecules* **1990**, *23*, 5234.
(43) Yasui, S. C.; Keiderling, T. A. *J. Am. Chem. Soc.* **1986**, *108*, 5576.
(44) Hermanns, Jr. J. *J. Phys. Chem.* **1966**, *70*, 510.
(45) Buhot, A.; Halperin, A. *Europhys. Lett.* **2000**, *50*, 756.

MA034093R